communications earth & environment

Article

https://doi.org/10.1038/s43247-024-01431-6

Northern Pacific sea-level pressure controls rain-on-snow in North America

Sinan Rasiya Koya, Kanak Kanti Kar & Tirthankar Roy ✉

Rain-on-snow (ROS) events, a phenomenon of liquid rainfall falling over accumulated snowpack, cause quick melting of snow, often leading to rapid and catastrophic flooding. Here we explore the causal drivers of ROS events across North America. A ROS identification method is proposed, which builds on the existing methods but adds more realism in terms of rain and snow conditions for ROS occurrence. We consider a wide range of observed hydrometeorological variables along with climatic oscillations over the period of 1951 to 2022. Causal linkages between the potential drivers and ROS frequency are explored by implementing Convergent Cross Mapping (CCM). Results suggest a strong causal link between the North-Pacific (NP) Index, a measure of sea-level pressure in the Northern Pacific Ocean, and ROS frequencies in North America, specifically in the eastern and western parts. We show the association of the NP index with the hydroclimatic variables and explain how this association might have contributed to this causal link. Thus, our findings provide valuable insights into the potential mechanisms of ROS events in different regions in North America.

A rain-on-snow (ROS) event refers to the hydrometeorological phenomena where rain falls onto an existing snowpack. Recently, ROS events have been of considerable societal importance as they cause destructive flooding[1,2], increase avalanche risk[3], disrupt transportation systems[4], damage infrastructure[5], and cause losses of ecosystem services[6,7]. Recent events such as the flash floods in Yellowstone National Park (in June 2022), the historic flood in the Midwestern US (in 2019 spring), and the crisis in Oroville Dam, CA (in 2017 spring) highlight the importance of considering ROS events in water resource management and planning[8–10]. Rapid snowmelt during ROS events can critically shift the hydrological cycle; as a result, groundwater recharge, river flow patterns, and water quality patterns can deteriorate[8]. These impacts hold great importance in North America, where 85 million people depend on rivers and reservoirs for the transportation and storage of water resources from mountain snow[11,12], which are susceptible to substantial flooding events caused by ROS[1,2,13–17].

Flooding is the most substantial consequence of ROS events[2]. Rapid snow melting due to the advected energy carried by rainfall and transferred to the existing snowpack can lead to a quick runoff and eventually a considerable river discharge within a short span of time[18–20]. Nevertheless, ROS events do not always result in flooding. Prior research has shown that comparable rainfall events can yield widely differing responses in snowpack runoff, contingent upon the prevailing hydroclimatic conditions[15,21,22]. Therefore, for operational flood forecasting, it is imperative to know the kind of rainfall events that can lead to more ROS-based flooding, which has also been considered as one of the 23 unsolved problems in hydrology[23].

Regardless of the disastrous impact of the ROS events, the mechanisms leading, i.e., the earth system processes causally associated with these events, are vaguely explored and mostly unknown. While precipitation can fall in the form of rain, snow, or mixed, two conditions are necessary for ROS to occur: 1) precipitation falling as rain, and 2) existing snowpack on the ground. Several studies showed the correlation between rainfall patterns and the earth system processes that drive them over North America[12,24–26]. Similarly, multiple studies explored the governing factors of the variability of snow over the continent[27–29]. However, these associations alone are insufficient for explaining the driving processes behind ROS events, as both rainfall and snowpack on the ground occurring independently cannot constitute a ROS event and thus cannot impact ROS frequency. Rather, we need to expand our understanding of processes in the earth system that can potentially result in the simultaneous occurrence of the two conditions mentioned above in order to examine ROS events. The prominence of these conditions (e.g., in some areas, the variability in the snowpack on the ground might be crucial to the ROS occurrence more than the fraction of precipitation falling as rain) and the hydrometeorological variables influencing them can vary across different regions. Moreover, the sensitive snow processes in a complex climate system[2,30] make understanding and predicting ROS events challenging. Although a handful of studies in the past have indicated the association of snow-related hydroclimatic variables and ROS in different regions[1,5,8,31–36], a larger-scale analysis based on observed records over the North American continent is lacking. Moreover, there could be unknown links between climatic patterns in the Earth system and the

Department of Civil and Environmental Engineering, University of Nebraska-Lincoln, Omaha, USA. ✉e-mail: roy@unl.edu

chances of ROS events on the continent. Specifically, understanding the causal links from the teleconnections would assist in better predicting imminent ROS probabilities, as their influence on the atmospheric circulation and hydrometeorological variables over the continent is well established[17,37–40]. The considerable impact of climate variation over the Pacific regions, such as the warming and cooling in the equatorial Pacific known as El Nino Southern Oscillation (ENSO), on the precipitation and temperature in the continent has been proven[25,39,40]. However, these relations between long-term climate oscillations and specific hydroclimatic variables, like precipitation or temperature, are insufficient to conclude their impact on ROS occurrences. This is because the ROS events are often not driven by a single variable influenced by the teleconnection but rather a combination of the states of different variables. For instance, precipitation during a persisting low temperature might not impact the chances of ROS events; instead, a short-term change in temperature and consequent snow-to-rain shift would increase the chances of ROS events[9].

While going through the studies investigating the drivers of ROS events, one can observe that almost all studies build their discussion based on the correlation between the variables and ROS events[1,32,34,41]. However, the three-century-old conundrum of "correlation vs. causation"-as appeared in "A Treatise on the Nature of Human Knowledge" by Bishop Berkeley in 1710- questions the approach adopted in these studies. In earth science alone, several variables have shown good correlations that are not dynamically coupled, often referred to as ephemeral or mirage correlation[42–44]. For instance, the abrupt warming in the extratropical Northern Hemisphere during the late 1980s was highly correlated to the Pacific Decadal Oscillation (PDO)-like pattern and the Arctic Oscillation (AO)-like pattern, which was later reported as a case of ephemeral correlation[43,45]. Therefore, to establish any association between different hydroclimatic phenomena, adopting methods that consider causality is a better choice.

In this study, we employ Convergent Cross Mapping (CCM)[45], a causal inference technique that assesses the extent to which two variables are integrated within a shared dynamic system (refer to the methods section for comprehensive details). Our aim is to delve into the fundamental hydroclimatic mechanism driving ROS events. We investigate the causal links between the teleconnection patterns, hydroclimatic variables, and ROS frequency. Using a newly proposed definition, we identify the ROS-evident regions in North America from the recorded measurements of hydroclimatic variables and analyze the trends and variability in ROS events across the continent. Our results expose different ROS-evident regions, where we check the causal links between the major teleconnection patterns around the North American continent and monthly ROS frequency. Our analysis led to the discovery of an interesting causal link between the sea-level pressure (SLP) in North Pacific[40] and monthly ROS frequency in North America. To further investigate the potential mechanism behind this direct causal link, we explored the causal influence of hydroclimatic variables on ROS events and how these variables are affected by North Pacific SLP. With the results of these experiments and existing domain knowledge, we could find substantial evidence to highlight the importance of the North Pacific SLP in the ROS occurrence in North America, which is discussed in the subsequent sections.

Results and Discussion

The analysis, based on our newly proposed ROS-day identification method, on recorded measurements of hydroclimatic variables from 1951 to 2022 across the North American Continent suggests that the ROS events are frequent in two regions: 1) American Northwest and Canadian Southwest, 2) American Northeast and Canadian Southeast (Fig. 1a). Unlike previous studies that have focused majorly on the Western US[1,2], possibly due to the availability of snow-related data and the importance of snow as a water resource in the region, our results point out that the Eastern US is an equally important region regarding ROS occurrence. In both of these regions, we observe seasonal differences in ROS occurrences. While most ROS days in the American Northwest and Canadian Southwest happened during the winter season (DJF; December-January-February), American Northeast and Canadian Southeast witnessed ROS days during spring (MAM; March-April-May) slightly higher than in winter (Fig. 1b, c). There were no major ROS days in the contiguous US during the Fall season (SON; September-October-November), though they were fairly frequent in the Canadian Southwest during the same time (Fig. 1d). Besides seasonal differences, we observed variability in ROS frequency relative to elevation (Fig. 1e). We can see that the ROS days were more common in the elevation range of 750 to 1250 meters from the mean sea level and reduced in higher or lower elevations (Fig. 1e). This could be related to the temperature in the mid-elevation range mostly staying around the freezing point of water, aiding the quick transitioning between rain and snow during a short span of time, thus increasing the likelihood of ROS, whereas, in higher or lower elevations, the temperature can be consistently colder or warmer, where an opposite effect might be apparent. At lower elevations, the median ROS frequency is higher during winter. However, as we go to higher elevations, the median ROS frequency is higher during spring. This is primarily attributable to lower temperatures in higher elevations, resulting in lower snow melting and, subsequently, a prolonged snow accumulation, which increases the chance of ROS when precipitation shifts to rainfall during warmer spring. Given the spatial and seasonal variability in ROS frequency, an inquisitive question to explore is what the potential drivers of these events are and, thus, their variability, starting from the climate system. In the subsequent sections, we discuss the insights from our study attempting to answer this question. Please note that we do not include the summer season in our analyses since ROS days rarely occur (near to zero across all elevation bands) during the summer season (JJA; June-July-August).

Teleconnections and ROS events

The mechanism behind the complex phenomena of ROS events has been an intriguing topic for the geoscientific research community. Through CCM, an algorithm to estimate the extent to which two time series are parts of a single dynamical system (refer to the methods section for comprehensive details), we explored the causal relationships between the teleconnection variables potentially relevant to North America and monthly ROS frequencies across 1346 stations. Out of all teleconnections, the North-Pacific (NP) Index - a measure of SLP in the region between 160°E to 140°W and 30°N to 65°N - shows a significant causal connection with ROS frequency (Fig. 2). Conversely, in almost all stations, CCM scores of the remaining teleconnection indices to ROS frequency are either not converging or nearly zero. These findings hold the same in the case of extreme ROS events (Fig. 3), where the rainfall causing ROS events is higher than 10 mm. That is, the NP index, in contrast with other teleconnections, shows a distinctive causal connection with extreme ROS frequency. At the same time, compared to all ROS events, the spatial extent of stations with high CCM scores (between NP and ROS frequency) is smaller in the case of extreme ROS events. This can be attributed to the fact that extreme ROS events are rare in occurrence (Supplementary Fig. 4). Compared to previous studies, which found significant correlations of ROS frequency with other teleconnection variables, such as AO, NAO, and ENSO[1,34], the outcome of our study can provide more insights for several reasons. Firstly, our study overcomes some of the consequential limitations of correlation-based analyses. Correlation cannot be a sufficient condition for causation, i.e., one phenomenon driving the other. Rather, correlation measures the co-occurrence of two events. For example, teleconnection variables are often linked to other physical processes in the Earth system, where both ROS frequency and teleconnections can be controlled by a common process (confounding factor). In such cases, we can expect a strong correlation between teleconnection and ROS frequency, and interpreting a direct relationship based on that would most likely be biased. Our findings indicate that, despite the observed correlations, no discernible causal links exist between the teleconnection variables and the ROS frequency, except for North Pacific SLP. This specific finding motivated us to explore how North Pacific SLP leads to ROS occurrence. For that reason, using CCM, we assessed two sets of causal connections in each station across North America: 1) the causal effect of hydroclimatic variables

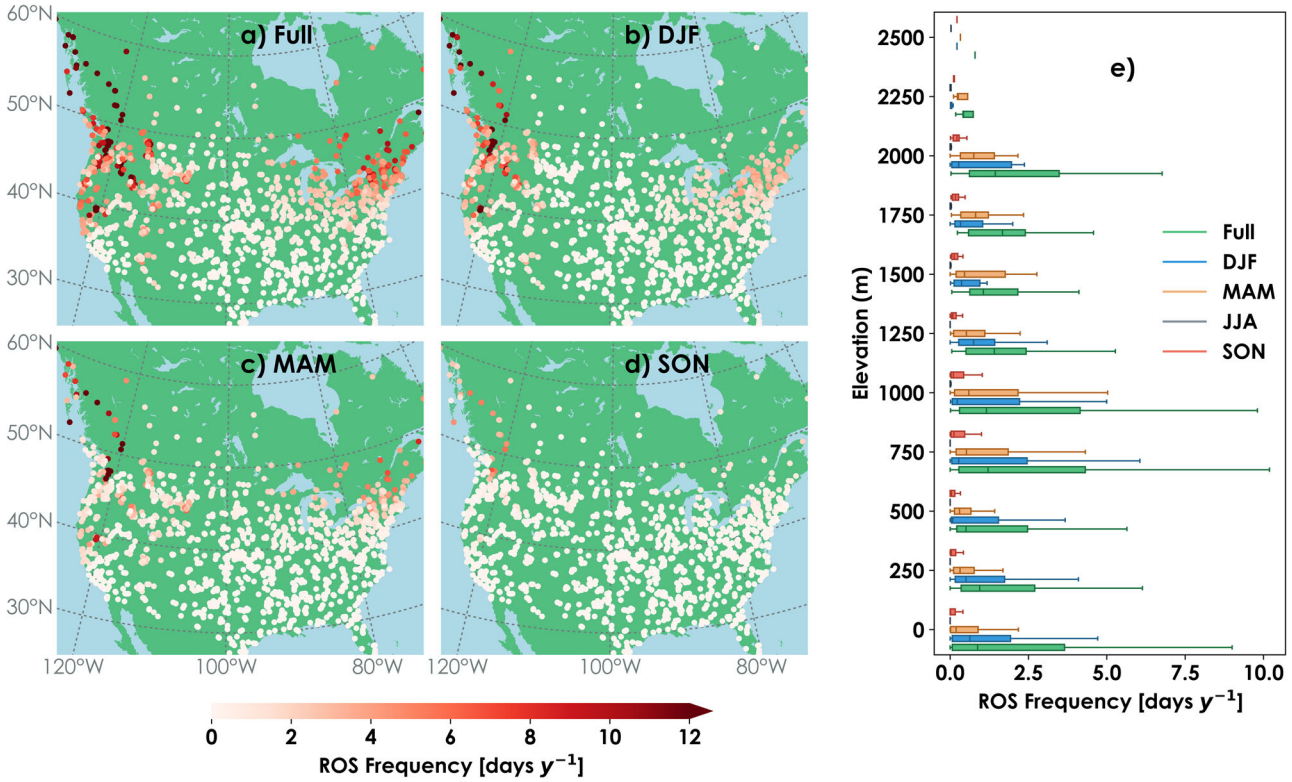

Fig. 1 | Frequency of ROS (days per year). a During full water year and (**b**–**d**) seasons and (**e**) their variability with respect to elevation from mean sea level.

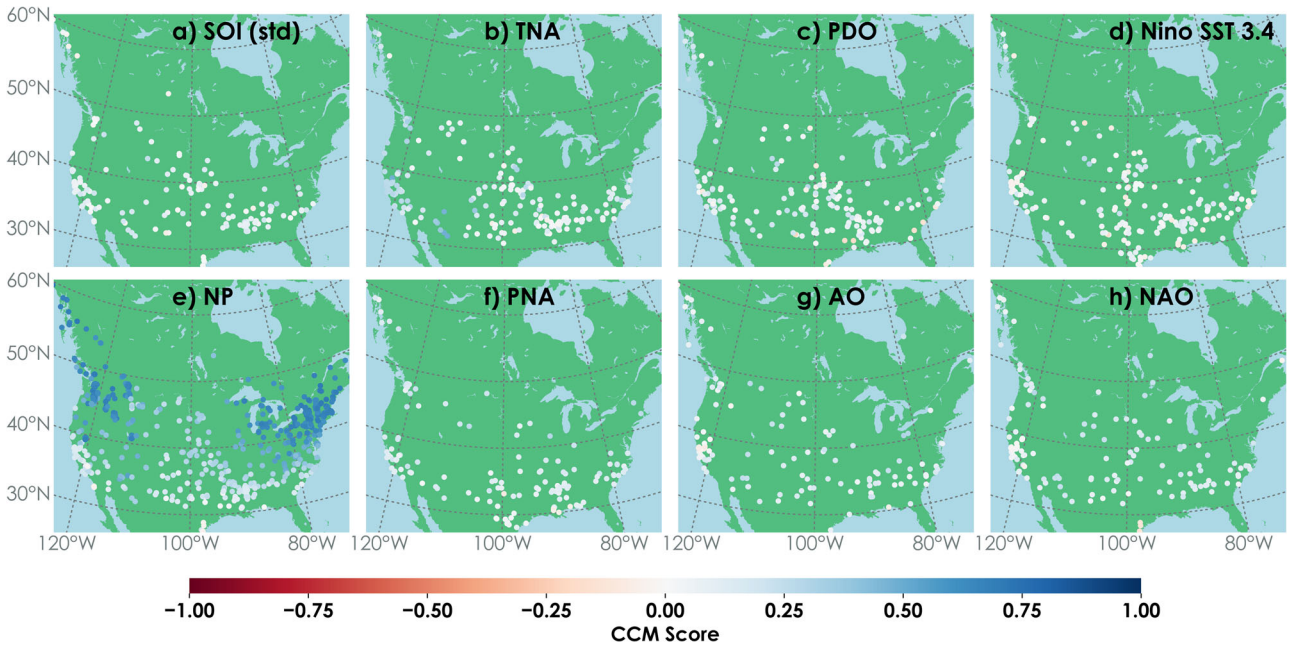

Fig. 2 | CCM scores of monthly teleconnection indices with ROS days per month. a Southern Oscillation Index (SOI). **b** Tropical North Atlantic (TNA) Index. **c** Pacific Decadal Oscillation (PDO) Index. **d** East Central Tropical Pacific Sea Surface Temperature (NINO SST 3.4). **e** North Pacific (NP) Index. **f** Pacific North American (PNA) Index. **g** Arctic Oscillation (AO). **h** North Atlantic Oscillation (NAO) Index. The higher (closer to +1) the value, the stronger the causal connection. Note that only stations where causality exists (i.e., stations where the CCM converges) are shown.

on ROS frequency and 2) the causal effect of North Pacific SLP on these hydroclimatic variables.

Causal effect of hydroclimatic variables on ROS frequency

To explore the causal connections of hydroclimatic variables with ROS occurrences, we estimated the CCM accuracy of several hydroclimatic variables with monthly ROS frequencies across all the stations (Fig. 4). Our results show, among the precipitation measures, a strong causation of snowfall followed by the total precipitation to ROS frequency in the American Northwest and Canadian Southwest (Fig. 4a, c). Their CCM accuracy is greater than that of rainfall in the region (Fig. 4b). Both these patterns can be observed in the case of extreme ROS events (Fig. 5a, b, and c).

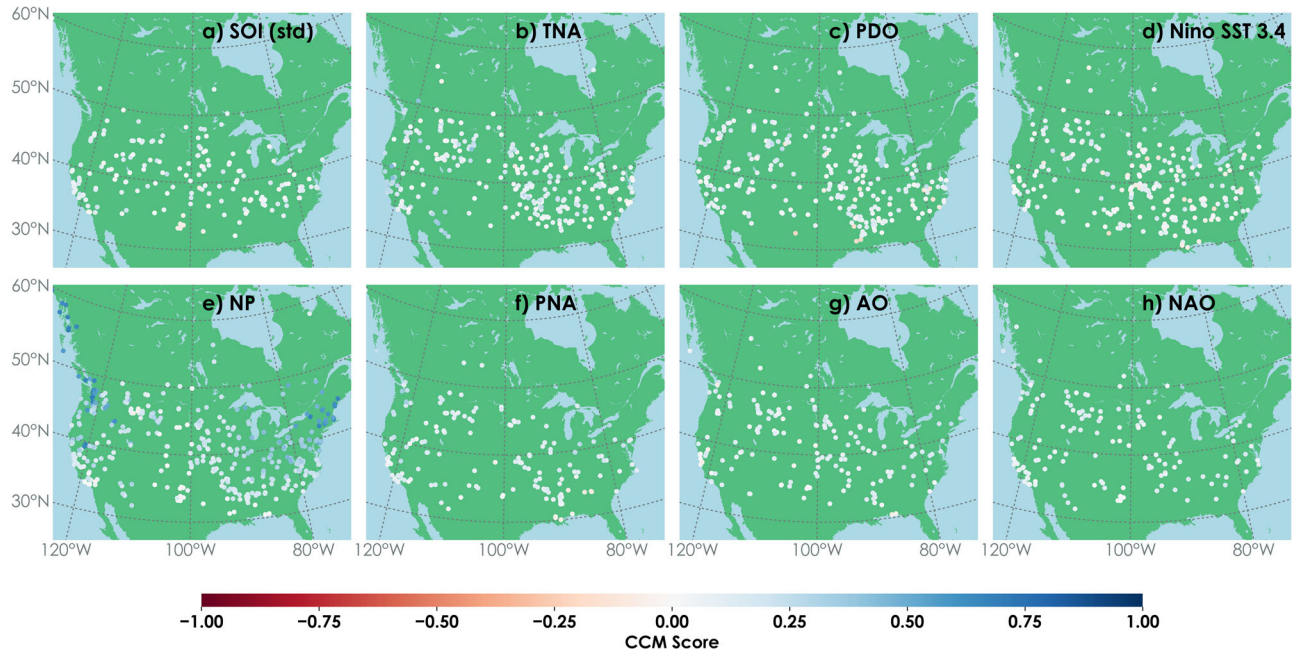

Fig. 3 | CCM scores of monthly teleconnection indices with extreme ROS days per month. a Southern Oscillation Index (SOI). **b** Tropical North Atlantic (TNA) Index. **c** Pacific Decadal Oscillation (PDO) Index. **d** East Central Tropical Pacific Sea Surface Temperature (NINO SST 3.4). **e** North Pacific (NP) Index. **f** Pacific North American (PNA) Index. **g** Arctic Oscillation (AO). **h** North Atlantic Oscillation (NAO) Index. The higher (closer to +1) the value, the stronger the causal connection. Note that only stations where causality exists (i.e., stations where the CCM converges) are shown.

Combined with high CCM accuracy for snow depth, this association suggests that snow accumulation might influence ROS occurrence more than liquid precipitation (shift to rainfall) in the American Northwest and Canadian Southwest. Here, additionally, we observe a higher CCM accuracy for diurnal temperature (near-surface) change to ROS frequency while considering all ROS events (Fig. 4h) as well as extreme ROS events (Fig. 5h). This suggests that quick temperature change and the consequent melting of fresh snow can be crucial in the ROS occurrence over the region. Unlike the American Northwest and Canadian Southwest, in stations in the American Northeast and Canadian Southeast, the influence of liquid precipitation is significant, as indicated by the CCM accuracies for rainfall to ROS frequency (Fig. 4b). Note that this association is slight in the case of extreme ROS events (Fig. 5b), most likely due to their lesser frequency in the region (Supplementary Fig. 4). Additionally, high CCM accuracies of monthly temperature variability to ROS frequency (Fig. 4i) indicate that a shift to liquid rainfall on later days is potentially causing ROS in the American Northeast and Canadian Southeast. Although lower in density, we can observe this effect with a lesser strength in case of extreme ROS events (Fig. 5i). The snowfall and snow depth show significant CCM accuracies in both ROS-evident regions (across all elevation ranges, Supplementary Fig. 5). This indicates that snow accumulation greatly influences ROS frequency, which is intuitive as the more snow on the ground, the higher the chances for ROS event. There is an interesting pattern in the CCM accuracies over the southwestern US (California). This region has a significant and high CCM score for snow depth compared to other hydroclimatic variables when considering all ROS frequency as well as extreme ROS frequency. The causal connection of snow depth to ROS frequency in the region (Figs. 4d, 5d), where it is comparatively warmer than other regions, indicates that the quick melting of snow is the likely reason for the reduced ROS frequency in the southwestern US. In both northeastern and northwestern parts of the US, CCM accuracies for temperature are significant and surpass that of other variables (Fig. 4g, h), suggesting a potential causal link that temperature controls the snowmelt rate and, thus, the likelihood of ROS events. Similarly, the mean snow fraction shows a strong causal connection with ROS frequency (Fig. 4e), indicating the importance of snow fraction as it is a direct measure of the occurrence of both snow and rain in a single month, which increases the chances of ROS. Both the effects of temperature and snow fraction are pertinent in the case of extreme ROS events (Fig. 5g–e).

Causal effect of North Pacific sea-level pressure on hydroclimatic variables

The CCM of the NP Index, representing North Pacific SLP, to the hydroclimatic variables in the stations, reveals several interesting patterns. The snowfall, snow depth, snow fraction, and mean temperature, which causally affect the ROS frequency in two major ROS-evident regions, are driven by North Pacific SLP (Fig. 6c,d,e,g). In the American Northeast and Canadian Southeast, the transition of precipitation between snow and rainfall has shown more importance, as discussed in the previous section. Our results demonstrate that the total precipitation has a noticeable absence of causal connection, whereas the rainfall and snowfall separately are causally affected by North Pacific SLP (Fig. 6a–c). This, along with the high CCM accuracy of North Pacific SLP to snow fraction (Fig. 6e), indicates the substantial influence of North Pacific SLP in determining the precipitation form (rain or snow) in the region, thus influencing the ROS frequency there. The potential reason behind this effect is the upper air temperature dipole between American Northeast and American Southwest and the subsequent gradient caused by North Pacific SLP, as established by Trenberth and Hurrell[40]. They show a significant negative correlation (-ve 60%) and a relatively lower positive correlation (+ve 30%) between the NP index and winter temperature at 700 hPa level. This indicates that the strengthening of the North Pacific SLP brings warmer temperatures from the Southeast towards the Northeast of the continent. This shift weakens with the weakening of the North Pacific SLP. The transition zone between the warmer and cooler regions goes through the American Northeast and Canadian Southeast. As an effect, the temperature shifts in winter over the region can be greatly controlled by the North Pacific SLP. Furthermore, the changes in the polar jet stream curvature due to high-pressure blockage in the North Pacific could affect the warm/cool transition of upper air over the region. Since the atmospheric waves must conserve the vorticity, the curvature in the jet stream caused by high pressure in the North Pacific likely propagates towards the continent, inducing a series of disturbances[46]. Consequently,

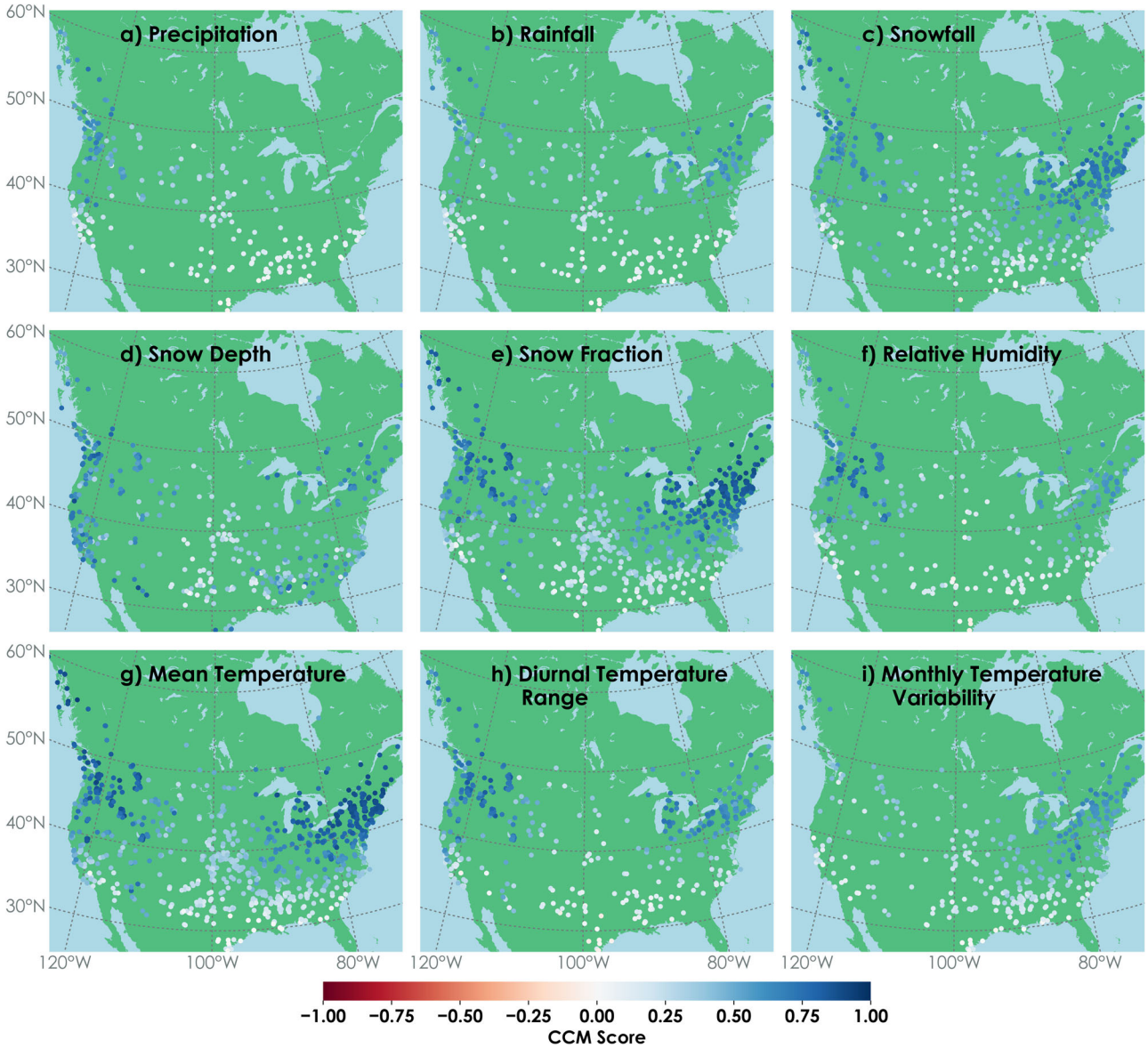

Fig. 4 | CCM score of monthly accumulated hydroclimatic variables to ROS days of the month. a Total precipitation including rainfall and snowfall. **b** Monthly accumulated rainfall. **c** Monthly accumulated snowfall. **d** Monthly average snowfall. **e** Monthly average snow fraction. **f** Monthly average relative humidity. **g** Monthly average of daily mean temperature. **h** Monthly average of diurnal temperature range. **i** Standard deviation of daily mean temperature. The higher (closer to +1) the value, the stronger the causal connection. Note that only stations where causality exists (i.e., stations where the CCM converges) are shown.

when there is high pressure in the North Pacific region, the polar jet becomes curvier, dragging cold air from the north and pushing the pre-existing warm air to the south. Douglas et al.[47] noted heavy cooling in the eastern half of the US during the high-pressure conditions in the North Pacific[47]. The opposite effect occurs when the pressure over the North Pacific is low. When these conditions interact with the moist air coming along the jet stream and from the Gulf of Mexico, they control the form of precipitation occurring. In essence, this back-and-forth effect with respect to the North Pacific SLP, where warmer and cooler conditions oscillate, could explain why it can be a deciding factor in the transition between snow and rain in the American Northeast, thus affecting the chances of ROS events. The relationship between North Pacific SLP and colder/warmer conditions in eastern North America was evident during the eastward shift of the North Pacific Oscillation index, which is derived from the North Pacific SLP, during 1995–2014[48]. Sung et al. (2019) found an increased probability of exceptionally warm (cool) winters during the positive (negative) phase of the North Pacific Oscillation, during which the North Pacific SLP is lower (higher) than normal[48]. Linkin and Nigam (2008) also reported the same association[49]. This teleconnection can be attributed to the observed changes to the Rossby waves during 1995–2014, which could propagate the eastern part of the North American continent through the northwestern part of Alaska. Furthermore, several case studies reveal a significant direct correlation between North Pacific and Northeastern America[50,51]. For example, Coleman and Rogers (2003) reported the association of the NP index with winter moisture conditions (+0.6 correlation between NP index and precipitation) in the Ohio River valley. One may note the absence of causal connections between Arctic Oscillation (AO)/North Atlantic Oscillation (NAO) and ROS frequency, regardless of their correlation shown by previous studies[34]. Besides the insufficiency of correlation to imply causation, this could be most likely because AO/NAO is majorly correlated with the snow cover in the Northeastern US, as noted by Cohen et al.[34]. However, our results suggest that snow cover is not the primary causal driver of ROS frequencies in the region. Moreover, Cohen et al.[34] found that the correlation on ROS frequency south of 60°N latitude is weak.

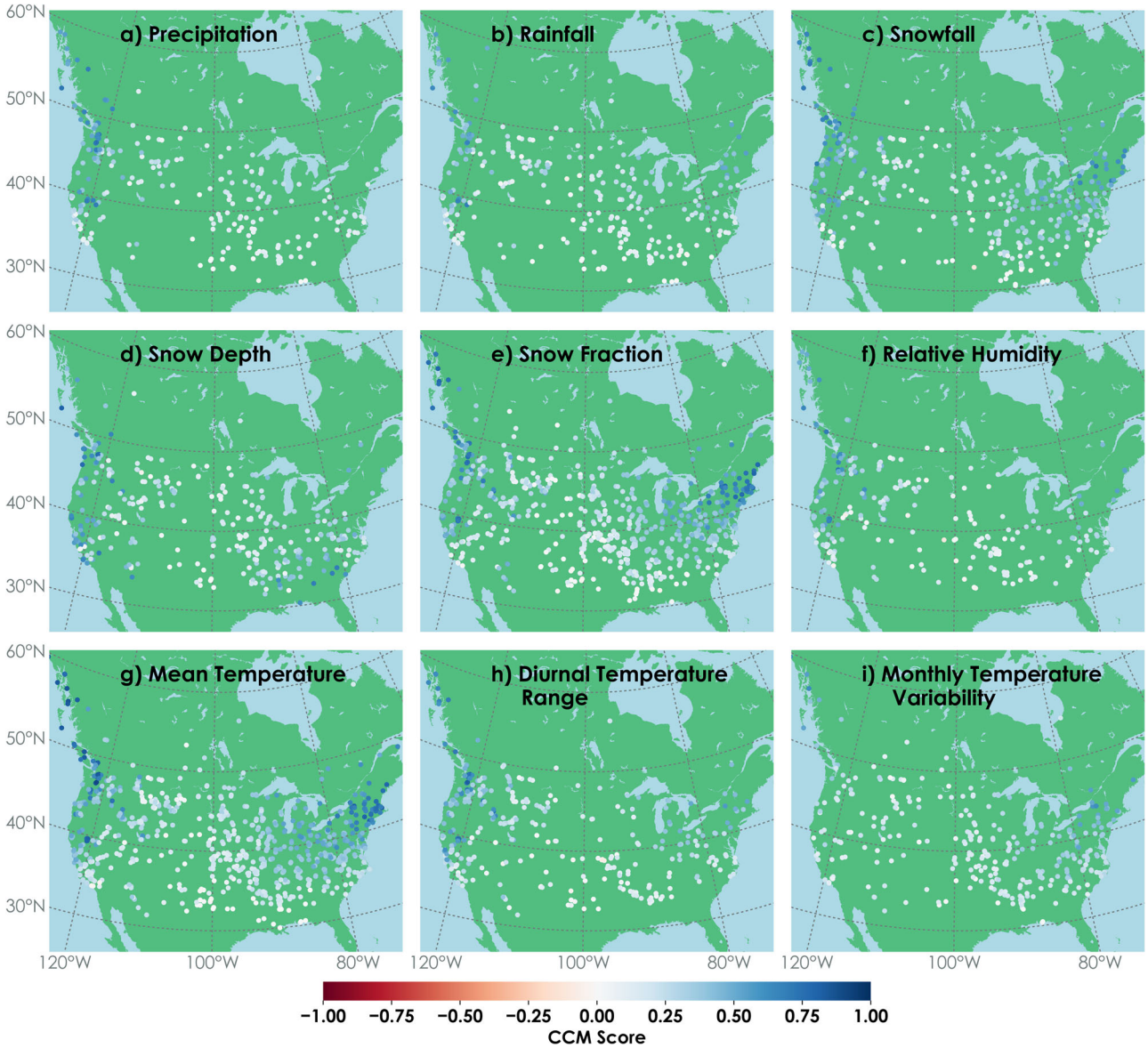

Fig. 5 | CCM score of monthly accumulated hydroclimatic variables to extreme ROS days. a Total precipitation including rainfall and snowfall. **b** Monthly accumulated rainfall. **c** Monthly accumulated snowfall. **d** Monthly average snowfall. **e** Monthly average snow fraction. **f** Monthly average relative humidity. **g** Monthly average of daily mean temperature. **h** Monthly average of diurnal temperature range. **i** Standard deviation of daily mean temperature. The higher (closer to +1) the value, the stronger the causal connection. Note that only stations where causality exists (i.e., stations where the CCM converges) are shown.

On the other side, in the American Northwest and Southwestern Canada, the CCM of hydroclimatic variables has revealed that snow accumulation drives ROS occurrence. Snowfall and snow depth in this region, indicating the snow accumulation, are likely influenced by North Pacific SLP, suggested by its high CCM accuracy with these variables (Fig. 6c, d). A higher North Pacific SLP facilitates snow accumulation due to its higher negative correlations with both surface and upper air temperature, as shown by Trenberth and Hurrell[40]. That is, during the higher North Pacific SLP, while the subsequent lower temperature in the upper air aids higher snowfall, the lower surface temperature decelerates the snow melt. Both these effects favor a higher snow accumulation, thus increasing the chances of ROS events in the region. Linkin and Nigam (2008) found a significant impact of variability in North Pacific SLP on the climate of the western part of the continent[49]. A lower-than-normal pressure in the North Pacific (enhanced NPO) might result in lower winter precipitation in Northwestern America and Southeastern Canada (this is attributed to the northward shift of storm tracks)[49]. Therefore, North Pacific SLP is crucial for the amount of winter precipitation, a variable that is causally connected with ROS frequency (Fig. 4a), in the region. The subsequent snow accumulation, received as a result of high winter precipitation, can be decisive in the likelihood of ROS. At the same time, the CCM scores of North Pacific SLP to the monthly temperature variability and rainfall in this region are low (Fig. 6b, i). The absence of this causal relation is dormant in influencing ROS days since these variables are not causally related to the ROS frequency in the region. Coming to the Southwestern US, the snow depth, which has shown higher CCM accuracy with ROS frequency (Fig. 6d), is not driven by the North Pacific SLP pattern. Therefore, North Pacific SLP might not be crucial for ROS occurrence there.

Although our study reveals how North Pacific pressure controls ROS occurrence in North America, similar causal connections can be potentially observed between ROS frequencies in other parts of the world and climate indices relevant to those regions. Previous studies have shown a significant correlation between ROS flooding in Germany and teleconnection patterns like NAO and Scandinavian Pattern[52,53]. Nied et al.[54] found a major

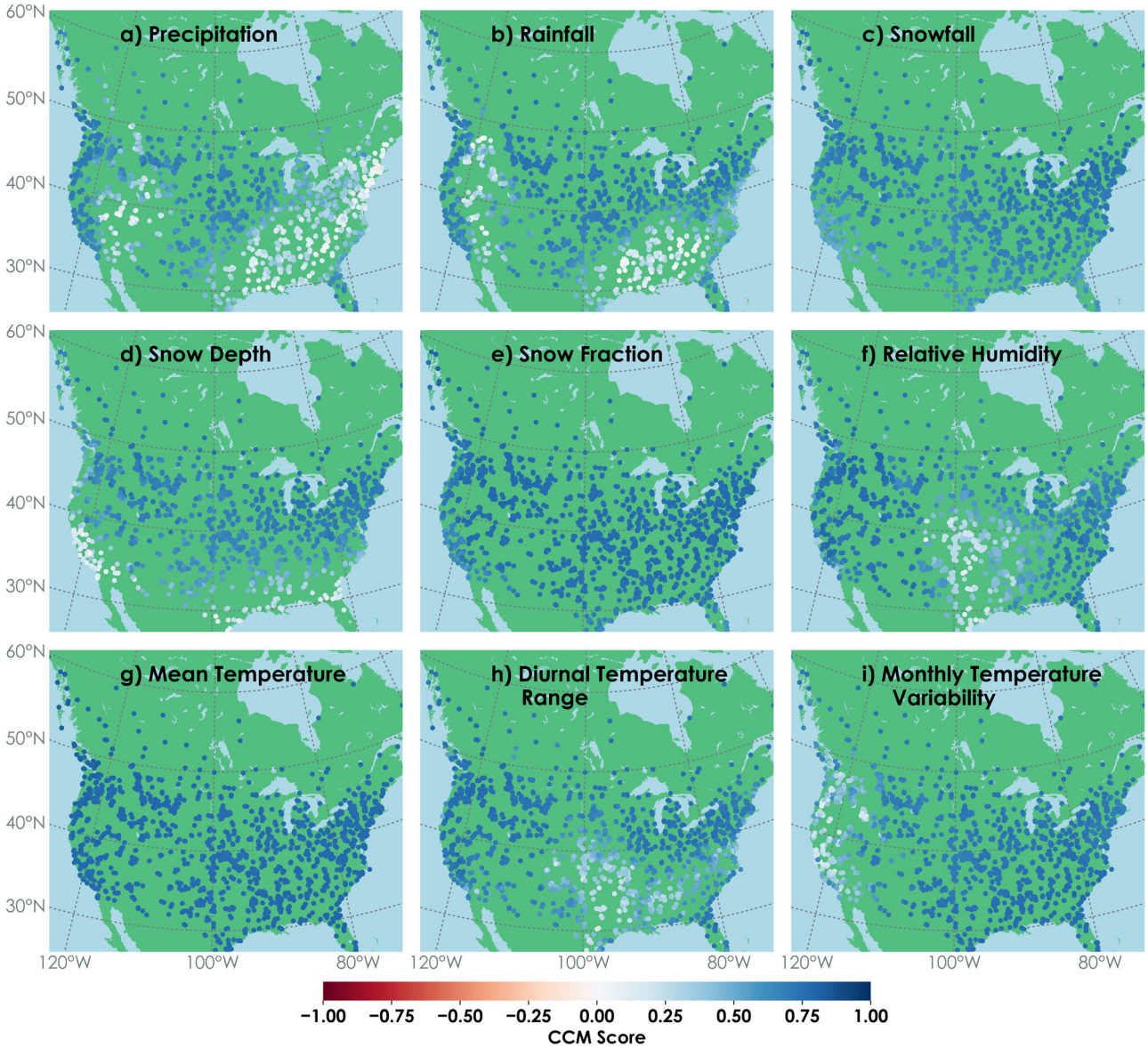

Fig. 6 | CCM score of North-Pacific index to monthly accumulated hydroclimatic variables. a Total precipitation including rainfall and snowfall. **b** Monthly accumulated rainfall. **c** monthly accumulated snowfall. **d** Monthly average snowfall. **e** Monthly average snow fraction. **f** Monthly average relative humidity. **g** Monthly average of daily mean temperature. **h** Monthly average of diurnal temperature range. **i** standard deviation of daily mean temperature. The higher (closer to +1) the value, the stronger the causal connection. Note that only stations where causality exists (i.e., stations where the CCM converges) are shown.

association between the ROS flooding in a European basin and westerly and northwesterly wind directions[54]. Since large-scale climate patterns can greatly influence these wind directions, similar to how North Pacific SLP influences the wind patterns over North America, it is very likely that significant causal connections exist between climate indices and ROS occurrence in Europe. However, extensive studies are required to establish such an association.

Trends

In light of potential drivers of ROS events in North America, we now examine the reasons behind the trends in ROS frequency during 1950-2022. We carried out the Mann-Kendall trend test (MK test) on the yearly time series of total ROS days during each water year and each season separately. As shown in Fig. 7a, the ROS frequency has both increasing and decreasing trends at different locations. In the Canadian Southwest, there is a decreasing trend in the total ROS days during the full water year, which is contributed by decreasing ROS days in the winter, spring, and fall seasons. This is most likely due to the decreasing trend in rainfall and snowfall during winter in that region (Fig. 8f, j), both reducing the likelihood of ROS events. Note that although there is an increasing trend in snow depth in a few stations, the influence of precipitation (as rain or snow) most likely surpasses that of snow depth. The decreasing trend in total ROS days in the full water year extends through the American Northwest. However, this decreasing trend is majorly contributed by the decreasing trend of total ROS days in winter (Fig. 7b) (consistent with the fact that this region witnesses most of the ROS days during winter). The decreasing trend is primarily attributable to the decreasing trend in winter snow depth and snowfall, as shown in Fig. 8j, since snow accumulation is the predominant driver of ROS events in the region. In addition, the rainfall also shows a decreasing trend in the region (Fig. 8f), which means a decreasing likelihood of ROS events. A similar phenomenon exacerbated by the decreasing trend in both rainfall and snowfall is the dry snow droughts in the upper western US, as reported by previous studies[55]. On the other side of the continent, most of the stations in the American Northeast and Canadian Southeast show a decreasing trend

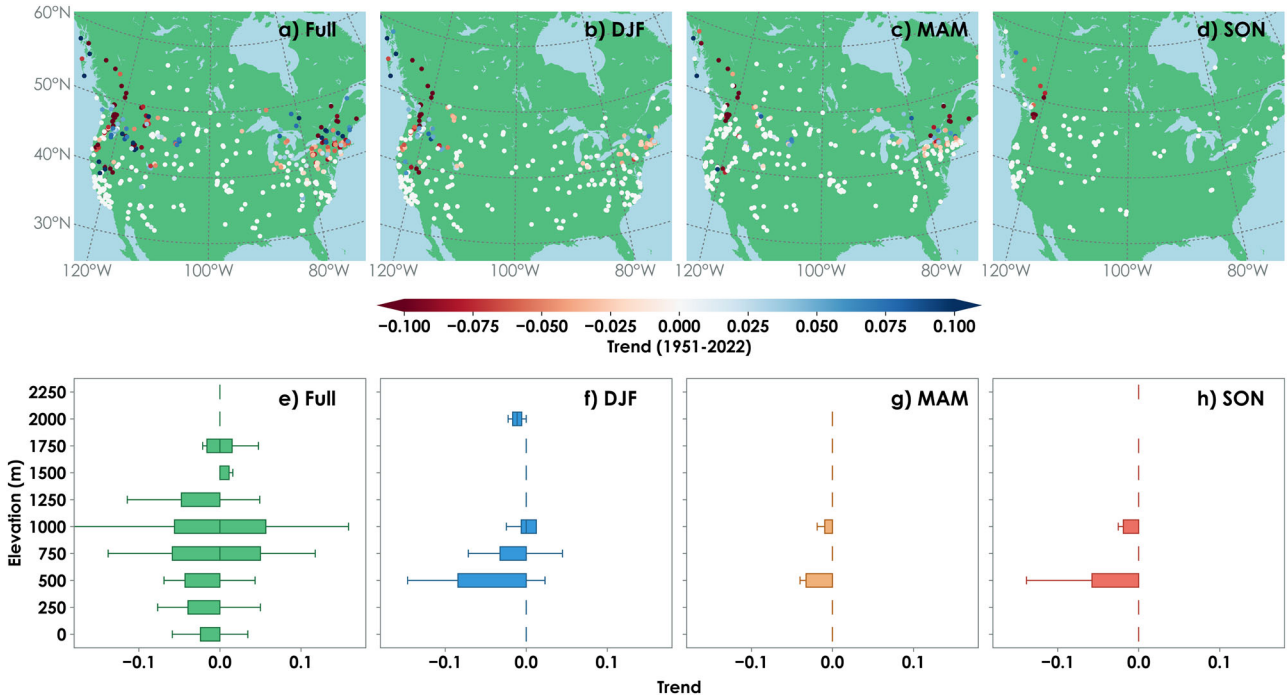

Fig. 7 | Trends in ROS frequency. Trends (Sen's slope) in (**a**) ROS days per full water year and (**b**–**d**) in each season. Variability in trends with respect to elevation (**e**–**h**). Note that only stations where a significant trend exists are shown.

mainly contributed by a decreasing trend in ROS days in spring seasons (Fig. 7c) (consistent with the fact that this region witnesses most of the ROS days during spring). The potential reason behind the decreasing trend in the eastern US is the decreasing trend in the snow depth during winter and spring (Fig. 8n, o) and the resulting reduction in the likelihood of ROS occurrence. In all stations in North America considered in this study, the increasing trends are majorly seen in elevation above 750 meters from the mean sea level (Fig. 7e). Across all seasons, we observe a majority of decreasing trends in ROS days in stations 500-750 meters from the mean sea level (Fig. 7f–h). There are no vital trends in total ROS seasonally across other elevation ranges.

It should be noted that in this study, we specifically look into ROS frequency; however, the magnitude of ROS events is equally important. Therefore, future research can focus on this specific aspect. Furthermore, we investigate the entire North American region, which gives us a comparative way of looking into ROS events across different sub-regions. We can see that certain regions, otherwise known to be ROS-prone (e.g., the Midwest), appear to be comparatively less impacted by ROS. This does not dilute the importance of ROS events in these regions. In fact, our approach can be adapted to specifically focus on these regions by making the ROS selection process less conservative (e.g., by changing the rain-snow partitioning scheme or thresholds used).

Conclusion

This study explores the causal drivers behind ROS events in North America and introduces a novel ROS-day identification method. We analyze the frequency and trends in ROS events in more than a thousand stations across the continent. We find the causal relationship of ROS frequency with teleconnections and hydroclimatic variables through CCM.

Our results show that the ROS days are frequent in mainly two regions: (1) American Northwest and Canadian Southwest, majorly during winter, and (2) American Northeast and Canadian Southeast, majorly during spring. In the former region, the ROS days are primarily driven by snow accumulation. Whereas, in the latter region, the shift of precipitation from rainfall to snowfall is the predominant driver of ROS days. Along with its influence on these factors, this study revealed a potential causal relationship between North Pacific SLP and the ROS occurrence in North America. Out of several teleconnections, the North-Pacific index, a measure of North Pacific SLP, showed a prominent influence on ROS frequency in the ROS-evident regions. Moreover, in these regions, the crucial hydroclimatic variables that potentially led to ROS days were heavily influenced by North Pacific SLP.

We observed decreasing trends in ROS days in most of the regions. While the decreasing trend in the Canadian Southwest was likely due to the decreasing trend in winter snowfall, the decreasing trend in snow depth is also a contributing factor in the American Northwest. On the other side, the decreasing trend in rainfall content in total precipitation is likely the key reason for the decreasing trend in ROS events in American Northeast and Canadian Southeast.

Methods

Data

We used the observed records of precipitation, temperature (minimum and maximum), and snow depth from the Global Historical Climatology Network-daily (GHCNd)[56–58]. GHCNd consists of over 100,000 stations across 180 countries, built upon integrating several land-based daily station records after a general quality control[59]. More details can be seen on the National Oceanic and Atmospheric Administration National Centers for Environmental Information (NOAA-NCEI) webpage (https://www.ncei.noaa.gov/products/land-based-station/global-historical-climatology-network-daily). We collected the dew point temperature from Integrated Surface Database (ISD)[60] summary of the day to derive the relative humidity, which we spatially joined (nearest station) with GHCNd dataset. It should be noted that most of the ISD and GHCNd stations overlap. We removed the stations with less than 30 years of records (out of period 1951-2022) of snow depth and dew point temperature (equivalent to less than 30 years of relative humidity records), resulting in 1346 stations in North America (Supplementary Fig. 1). Most of these stations are within the contiguous US and southern Canada. All these stations have more than 30 years of records of remaining variables used in this study, discarding the necessity of further filtering by length of records. Although the above-mentioned datasets are published after regular quality control, we did the following additional steps

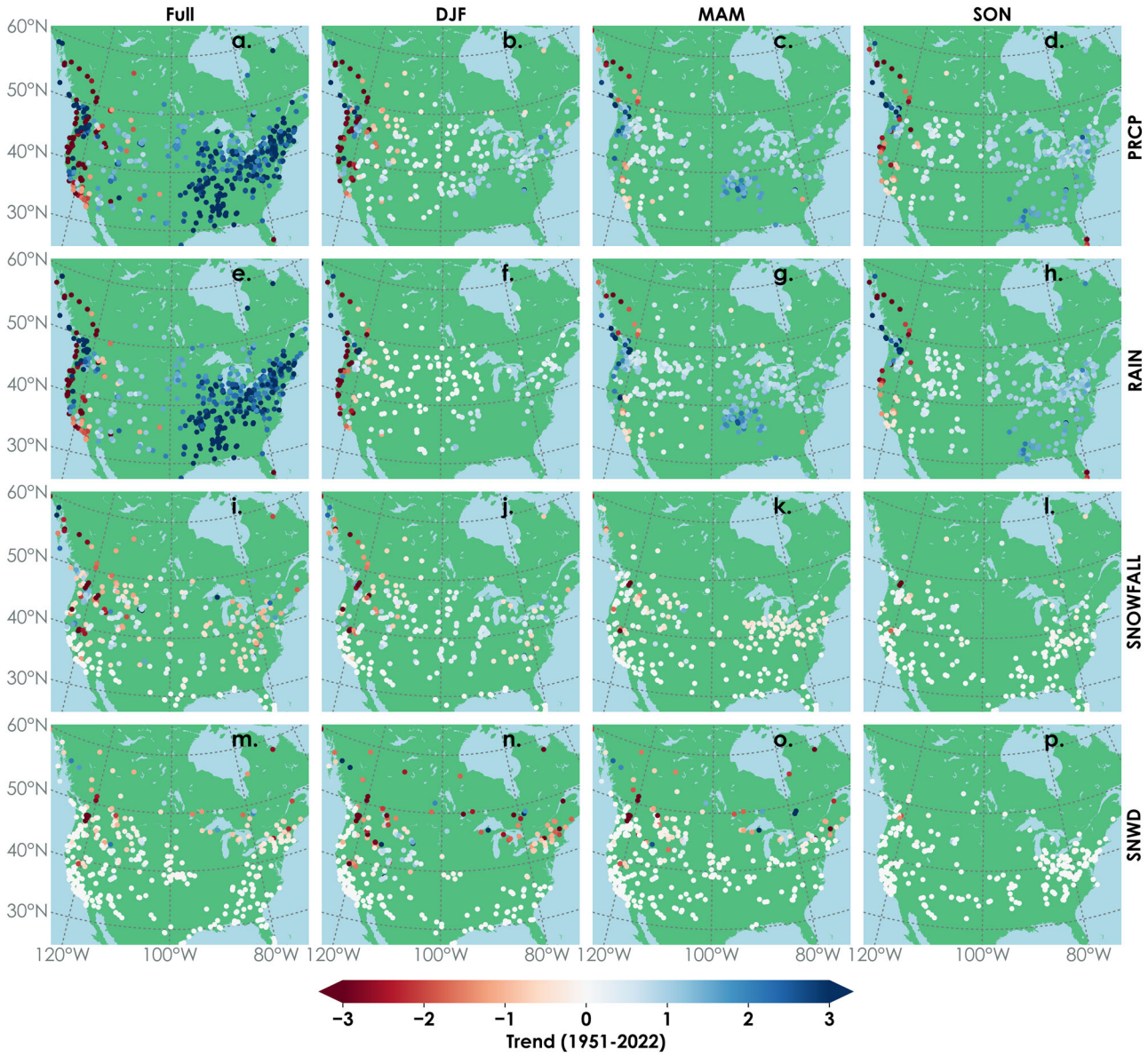

Fig. 8 | Trends in hydrometeorological variables. Trends (Sen's slope) in (**a**–**d**) accumulated precipitation, (**e**–**h**) accumulated rainfall, (**i**–**l**) accumulated snowfall, and (**m**–**p**) average snow depth during (a, e, **i**, **m**) full water year, (**b**, **f**, **j**, **n**) December–January–February (**c**, **g**, **k**, **o**) March–April–May (**d**, **h**, **l**, **p**) September–October–November. Note that only stations where a significant trend exists are shown.

to ensure the best consistency of the dataset for the analyses in this study. We removed records with (1) erroneous extreme values of temperature (outside [−70, 60] °C), precipitation (outside [0,3000] mm), and snow depth (outside [0,30000] mm), (2) internal inconsistencies in temperature (min. temperature greater than max. temperature), (3) excessive diurnal temperature change (more than 40 °C), (4) extreme erroneous temperature spikes (more than 60 °C). Subsequently, the missing data for each day is filled using the k-Nearest Neighbors (kNN) method. We used eight neighboring stations with inverse distance weights to fill a missing record of a station. Furthermore, to study the linkage between teleconnections and ROS events, we collected the monthly timeseries from 1951 to 2022 (complete and continuous) of teleconnection indices (Supplementary Table 1) from the NOAA Physical Science Laboratory (NOAA-PSL) website (https://psl.noaa.gov/data/climateindices/list/).

Methodology

We define a daily ROS event (or a ROS Day) as a day with higher than 1 mm of rainfall (liquid precipitation) falling over 10 mm of snow depth. The 1 mm threshold for rainfall is used to eliminate drizzle. The 10 mm minimum snow depth is chosen because it is the lowest recorded snow depth. Moreover, snow depth is generally recorded to the nearest whole inch, and a snow depth of 0.4 inches (10.16 mm) or below would be recorded as trace[61–63]. The amount of rainfall in total precipitation is calculated through the wet bulb temperature-based rain-snow partitioning scheme proposed by Wang et al. (Supplementary Fig. 2)[64]. This sigmoid functions-based scheme, which has been implemented in popular land surface models Noah-MP and HLM, is proven to be identical to the measured snow fraction[35,64,65].

Our ROS event selection is advantageous over existing ROS Days definitions for multiple reasons. We use ground-based measurements to carry out our analysis. Using reanalysis or model data to identify ROS events, as in several previous studies[34,66–69], consists of errors and biases introduced by the model. In contrast, station-based observations are more accurate and generally regarded as ground truth. We eliminate the dependency of ROS Day definition on manually decided thresholds. Previous studies based on observed records[1] defined ROS Day as a day with positive precipitation and snow depth reduced from the previous day. This can be

problematic as it includes days with smaller or erroneous values of precipitation (drizzles) and snow depth, leading to incorrect identification of ROS days. This is evident in Supplementary Fig. 3 (first row), which shows unlikely ROS frequency when a condition of positive precipitation is used. The solution for this issue is to enforce a threshold for snow depth and precipitation. However, the thresholds adopted in the later studies[2,70,71] are often based on expert judgments, which are subjective. In comparison, our definition eliminates chances of subjectivity by imposing the logical conditions following steps of the physical process ROS, i.e., estimating the rainfall in total precipitation and checking whether it is falling over the minimum recorded snow depth. To further affirm that our ROS Day definition is independent of threshold, we show the variability of ROS frequency (ROS days per year) with respect to different thresholds for snow depth and rainfall (Supplementary Fig. 3). The ROS frequency remains nearly the same as we change the snow depth threshold. Whereas the ROS frequency reduces as the threshold for rainfall increases, which is intuitive as the higher the threshold, the more rainfall events are removed. Since we apply a threshold only after filtering the rainfall content in total precipitation, we do not need to enforce a threshold other than removing the drizzle, staying as close as possible to the physical occurrence of ROS events in the real world. However, the ROS events selected based on the above criteria include both weaker and extreme ROS events. Therefore, to study the extreme ROS events, which could potentially yield a flood, we filtered those ROS days with rainfall higher than 10 mm (based on Musselman et al.[2]). The analyses are conducted on both categories, i.e., all ROS events and extreme ROS events separately.

Our definition is wholly based on observed variables, enabling us to identify ROS events from the records. Previous studies carried out ROS analyses based on model-simulated snowmelt, which is nearly impossible to measure in the real world[2,14]. Thus, such definitions can be susceptible to model errors and forcing measurement errors. Moreover, earth system model simulations are often computationally intensive. The variables used in our definition (precipitation, temperature, snow depth, and relative humidity) are recorded worldwide frequently as station, radar, and satellite measurements. In case of missing relative humidity records, it can be derived from other recorded variables like dew point temperature or specific humidity.

In this study, the frequency of ROS days refers to the total number of ROS days per full water year (Oct-Sep) or specific period (e.g., seasons) of the water year. It is calculated as total ROS days divided by the total number of water years in the time series. Similarly, seasonal frequencies are calculated as total ROS days belonging to a season divided by the total number of that season in the time series. The trend in the time series of ROS frequency and GHCNd variables is calculated using the Mann–Kendall trend test[72,73]. We only reported the Sen's slope of stations where the MK test identified the existence of a significant trend.

Among the limited number of studies in the literature exploring the hydroclimatic drivers of ROS events, almost all examined the correlation between the potential drivers and ROS frequency. However, correlation can be misguiding as it does not imply a causal connection between driver and effect[45]. To investigate the intriguing question of what *causes* ROS events, we use CCM to discover such existing causal connections between hydroclimatic variables and monthly ROS frequency. CCM is based on the dynamical systems theory, which says that two-time series are causally related if they share a single dynamic system, which can be represented by an attractor manifold (e.g., Lorenz attractor). In essence, CCM tries to reproduce the time series of the effecting variable from that of the causing variable through the shadow manifolds of an unknown dynamical system[45,74]. The accuracy between the actual and reproduced time series indicates causality. In this study, we use the Pearson correlation coefficient to measure this accuracy (referred as CCM accuracy or score in this article). In CCM, we construct an attractor in an n-dimensional space from an n-lagged time series. In other words, we can trace the lagged time series as the projection of the attractor. Since we run CCM with monthly time series in our study, we embed the time series in a 12-dimensional space as it ensures that at least a full-year lag of time series is used to construct the attractor. The lag amount is estimated as the minimum lag before the mutual information between the time series and the lagged time series increases. As this is a maximum lag before obtaining any new information, it ensures we do not lose any information when embedding the time series in an n-dimensional space. We must check for the convergence of CCM accuracy as the time series length increases to conclude a causal relationship. For that, we check that the CCM accuracies of the ten longest periods of two time series of interest do not deviate more than 0.01 ($|X_{t+1} - X_t| < 0.01$, for all $t \geq L - 10$, where L is the time series length, and X is the CCM accuracy). For more details about the algorithm, please see Sugihara et al.[45].

Data availability

The dataset used in this study, Global Historical Climatology Network-daily (GHCNd), is publicly provided by the National Centers for Environmental Information (NCEI) and can be accessed from https://www.ncei.noaa.gov/products/land-based-station/global-historical-climatology-network-daily. The results data and final figures obtained from our analysis can be found at https://doi.org/10.5281/zenodo.10956598[75].

Code availability

Codes used in this study can be found at https://doi.org/10.5281/zenodo.10956598[75].

Received: 1 December 2023; Accepted: 30 April 2024;
Published online: 16 May 2024

References

1. McCabe, G. J., Clark, M. P. & Hay, L. E. Rain-on-snow events in the western United States. *Bull. Am. Meteorol. Soc.* **88**, 319–328 (2007).
2. Musselman, K. N. et al. Projected increases and shifts in rain-on-snow flood risk over western North America. *Nat. Clim. Chang.* **8**, 808–812 (2018).
3. Schweizer, J., Jamieson, J. B. & Schneebeli, M. Snow avalanche formation. *Rev. Geophys*. **41**, (2003).
4. Putkonen, J. & Roe, G. Rain-on-snow events impact soil temperatures and affect ungulate survival. *Geophys. Res. Lett.* **30**, 1–4 (2003).
5. Hansen, B. B. et al. Warmer and wetter winters: characteristics and implications of an extreme weather event in the High Arctic. *Environ. Res. Lett.* **9**, 114021 (2014).
6. Rennert, K. J., Roe, G., Putkonen, J. & Bitz, C. M. Soil thermal and ecological impacts of rain on snow events in the circumpolar arctic. *J. Clim.* **22**, 2302–2315 (2009).
7. Putkonen, J. et al. Rain on snow: little understood killer in the North. *Eos, Trans. Am. Geophys. Union* **90**, 221–222 (2009).
8. Flanagan, P. X. et al. A hydrometeorological assessment of the historic 2019 Flood of Nebraska, Iowa, and South Dakota. 817–829 (2019).
9. Michaelis, A. C. et al. Atmospheric river precipitation enhanced by climate change: a case study of the storm that contributed to California's Oroville Dam crisis. *Earth's Futur* **10**, e2021EF002537 (2022).
10. Yellowstone flooding: Why is it happening now? https://www.nationalgeographic.com/environment/article/yellowstone-flooding-why-is-it-happening-now.
11. Sturm, M., Goldstein, M. A. & Parr, C. Water and life from snow: a trillion dollar science question. *Water Resour. Res.* **53**, 3534–3544 (2017).
12. Barnett, T. P., Adam, J. C. & Lettenmaier, D. P. Potential impacts of a warming climate on water availability in snow-dominated regions. *Nature* **438**, 303–309 (2005).
13. Kattelmann, R. Flooding from rain-on-snow events in the Sierra Nevada. *IAHS Publ. Proc. Rep.-Intern Assoc. Hydrol. Sci.* **239**, 59–66 (1997).
14. Marks, D., Link, T., Winstral, A. & Garen, D. Simulating snowmelt processes during rain-on-snow over a semi-arid mountain basin. *Ann. Glaciol.* **32**, 195–202 (2001).

15. Kroczynski, S. A comparison of two rain-on-snow events and the subsequent hydrologic responses in three small river basins in central Pennsylvania (2004).
16. Brunengo, M. J. A method of modeling the frequency characteristics of daily snow amount, for stochastic simulation of rain-on-snowmelt events. *Proc. Western Snow Conf*. **58**, 110–121 (1990).
17. Leathers, D. J., Kluck, D. R. & Kroczynski, S. The severe flooding event of january 1996 across North-Central Pennsylvania. *Bull. Am. Meteorol. Soc.* **79**, 785–798 (1998).
18. Harr, R. D. Some characteristics and consequences of snowmelt during rainfall in western Oregon. *J. Hydrol.* **53**, 277–304 (1981).
19. Berris, S. N. & Harr, R. D. Comparative snow accumulation and melt during rainfall in forested and clear-cut plots in the Western Cascades of Oregon. *Water Resour. Res.* **23**, 135–142 (1987).
20. Pomeroy, J. W., Fang, X. & Marks, D. G. The cold rain-on-snow event of June 2013 in the Canadian Rockies—characteristics and diagnosis. *Hydrol. Process.* **30**, 2899–2914 (2016).
21. Cline, D. W. Snow surface energy exchanges and snowmelt at a continental, midlatitude Alpine site. *Water Resour. Res.* **33**, 689–701 (1997).
22. Marks, D. & Dozier, J. Climate and energy exchange at the snow surface in the Alpine Region of the Sierra Nevada: 2. Snow cover energy balance. *Water Resour. Res.* **28**, 3043–3054 (1992).
23. Blöschl, G. et al. Twenty-three unsolved problems in hydrology (UPH) —a community perspective. *Hydrol. Sci. J.* **64**, 1141–1158 (2019).
24. Ombadi, M., Risser, M. D., Rhoades, A. M. & Varadharajan, C. A warming-induced reduction in snow fraction amplifies rainfall extremes. *Nature* **619**, 305–310 (2023).
25. Leathers, D. J., Yarnal, B. & Palecki, M. A. The Pacific/North American teleconnection pattern and United States climate. Part I: Regional temperature and precipitation associations. *J. Clim.* **4**, 517–528 (1991).
26. Ning, L. & Bradley, R. S. Winter precipitation variability and corresponding teleconnections over the northeastern United States. *J. Geophys. Res.* **119**, 7931–7945 (2014).
27. Ghatak, D., Gong, G. & Frei, A. North American temperature, snowfall, and snow-Depth response to winter climate modes. *J. Clim.* **23**, 2320–2332 (2010).
28. Mote, P. W., Li, S., Lettenmaier, D. P., Xiao, M. & Engel, R. Dramatic declines in snowpack in the western US. *npj Clim. Atmos. Sci*. **1**, (2018).
29. Zeng, X., Broxton, P. & Dawson, N. Snowpack change from 1982 to 2016 over conterminous United States. *Geophys. Res. Lett*. **45**, 12–940 (2018).
30. O'Gorman, P. A. Contrasting responses of mean and extreme snowfall to climate change. *Nature* **512**, 416–418 (2014).
31. Pan, C. G., Kirchner, P. B., Kimball, J. S., Kim, Y. & Du, J. Rain-on-snow events in Alaska, their frequency and distribution from satellite observations. *Environ. Res. Lett*. **13**, (2018).
32. Ye, H., Yang, D. & Robinson, D. Winter rain on snow and its association with air temperature in northern Eurasia. *Hydrol. Process.* **22**, 2728–2736 (2008).
33. Pall, P., Tallaksen, L. M. & Stordal, F. A climatology of rain-on-snow events for Norway. *J. Clim.* **32**, 6995–7016 (2019).
34. Cohen, J., Ye, H. & Jones, J. Trends and variability in rain-on-snow events. *Geophys. Res. Lett.* **42**, 7115–7122 (2015).
35. Rasiya Koya, S. et al. Applicability of a flood forecasting system for Nebraska watersheds. *Environ. Model. Softw.* **164**, 105693 (2023).
36. Velásquez, N., Quintero, F., Koya, S. R., Roy, T. & Mantilla, R. Snow-detonated floods: Assessment of the U.S. midwest March 2019 event. *J. Hydrol. Reg. Stud.* **47**, 101387 (2023).
37. Sheridan, S. C. North American weather-type frequency and teleconnection indices. *Int. J. Climatol.* **23**, 27–45 (2003).
38. Ge, Y. & Gong, G. North American snow depth and climate teleconnection patterns. *J. Clim.* **22**, 217–233 (2009).
39. Mccabe, G. J., Ault, T. R., Cook, B. I., Betancourt, J. L. & Schwartz, M. D. Influences of the El Niño Southern Oscillation and the pacific decadal oscillation on the timing of the North American spring. *Int. J. Climatol.* **32**, 2301–2310 (2012).
40. Trenberth, K. E. & Hurrell, J. W. Decadal atmosphere-ocean variations in the Pacific. *Clim. Dyn.* **9**, 303–319 (1994).
41. Pradhanang, S. M. et al. Rain-on-snow runoff events in New York. *Hydrol. Process.* **27**, 3035–3049 (2013).
42. Rodó, X., Pascual, M., Fuchs, G. & Faruque, A. S. G. ENSO and cholera: A nonstationary link related to climate change? *Proc. Natl. Acad. Sci. USA* **99**, 12901–12906 (2002).
43. Lo, T. T. & Hsu, H. H. Change in the dominant decadal patterns and the late 1980s abrupt warming in the extratropical Northern Hemisphere. *Atmos. Sci. Lett.* **11**, 210–215 (2010).
44. Mysterud, A., Stenseth, N. C., Yoccoz, N. G., Langvatn, R. & Steinheim, G. Nonlinear effects of large-scale climatic variability on wild and domestic herbivores. *Nature* **410**, 1096–1099 (2001).
45. Sugihara, G. et al. Detecting causality in complex ecosystems. *Science* **338**, 496–500 (2012).
46. Trenberth, K. E. Recent observed interdecadal climate changes in the Northern Hemisphere. *Bull. Am. Meteorol. Soc.* **71**, 988–993 (1990).
47. Douglas, A. V., Cayan, D. R. & Namias, J. Large-scale changes in North Pacific and North American weather patterns in recent decades. *Mon. Weather Rev.* **110**, 1851–1862 (1982).
48. Sung, M.-K. et al. Tropical influence on the North Pacific Oscillation drives winter extremes in North America. https://doi.org/10.1038/s41558-019-0461-5.
49. Linkin, M. E. & Nigam, S. The North Pacific Oscillation–West Pacific Teleconnection Pattern: mature-phase structure and winter impacts. *J. Clim.* **21**, 1979–1997 (2008).
50. Coleman, J. S. M. & Rogers, J. C. Ohio River Valley winter moisture conditions associated with the Pacific–North American Teleconnection Pattern. *J. Clim.* **16**, 969–981 (2003).
51. Schulte, J. A., Najjar, R. G. & Li, M. The influence of climate modes on streamflow in the Mid-Atlantic region of the United. *States. J. Hydrol. Reg. Stud.* **5**, 80–99 (2016).
52. Krug, A., Primo, C., Fischer, S., Schumann, A. & Ahrens, B. On the temporal variability of widespread rain-on-snow floods. *Meteorol. Zeit.* **29**, 147–163 (2020).
53. Tarasova, L., Ahrens, B., Hoff, A. & Lall, U. The value of large-scale climatic indices for monthly forecasting severity of widespread flooding using dilated convolutional neural networks. *Earth's Futur*. **12**, (2024).
54. Nied, M. et al. On the relationship between hydro-meteorological patterns and flood types. *J. Hydrol.* **519**, 3249–3262 (2014).
55. Harpold, A. A., Dettinger, M. & Rajagopal, S. Defining snow drought and why it matters. *Eos* **98**, https://doi.org/10.1029/2017EO068775 (2017).
56. Menne, M. J., Durre, I., Vose, R. S., Gleason, B. E. & Houston, T. G. An overview of the global historical climatology network-daily database. *J. Atmos. Ocean. Technol.* **29**, 897–910 (2012).
57. Durre, I., Menne, M. J., Gleason, B. E., Houston, T. G. & Vose, R. S. Comprehensive automated quality assurance of daily surface observations. *J. Appl. Meteorol. Climatol.* **49**, 1615–1633 (2010).
58. Durre, I., Menne, M. J. & Vose, R. S. Strategies for evaluating quality assurance procedures. *J. Appl. Meteorol. Climatol.* **47**, 1785–1791 (2008).
59. Global Historical Climatology Network daily (GHCNd) | National Centers for Environmental Information (NCEI). https://www.ncei.noaa.gov/products/land-based-station/global-historical-climatology-network-daily.
60. Smith, A., Lott, N. & Vose, R. The integrated surface database: recent developments and partnerships. *Bull. Am. Meteorol. Soc.* **92**, 704–708 (2011).
61. National Weather Service. Snow Measurement Guidelines for National Weather Service Surface Observing Programs. National Weather Service. https://www.weather.gov/media/coop/Snow_Measurement_Guidelines- 2014.pdf (2013).

62. National Weather Service. Snow Measurement Guidelines for National Weather Service Snow Spotters. https://www.weather.gov/media/ffc/snow_measurement_guidelines.pdf (2012).
63. Snow Measurement Guidelines. https://www.weather.gov/gsp/snow.
64. Wang, Y. H. et al. A wet-bulb temperature-based rain-snow partitioning scheme improves snowpack prediction over the Drier Western United States. *Geophys. Res. Lett.* **46**, 13825–13835 x(2019).
65. Behrangi, A., Yin, X., Rajagopal, S., Stampoulis, D. & Ye, H. On distinguishing snowfall from rainfall using near-surface atmospheric information: Comparative analysis, uncertainties and hydrologic importance. *Q. J. R. Meteorol. Soc.* **144**, 89–102 (2018).
66. Il Jeong, D. & Sushama, L. Rain-on-snow events over North America based on two Canadian regional climate models. *Clim. Dyn.* **50**, 303–316 (2018).
67. Bieniek, P. A. et al. Assessment of Alaska rain-on-snow events using dynamical downscaling. *J. Appl. Meteorol. Climatol.* **57**, 1847–1863 (2018).
68. Crawford, A. D., Alley, K. E., Cooke, A. M. & Serreze, M. C. Synoptic climatology of rain-on-snow events in Alaska. *Mon. Weather Rev.* **148**, 1275–1295 (2019).
69. López-Moreno, J. I. et al. Changes in the frequency of global high mountain rain-on-snow events due to climate warming. *Environ. Res. Lett.* **16**, 094021 (2021).
70. Freudiger, D., Kohn, I., Stahl, K. & Weiler, M. Large-scale analysis of changing frequencies of rain-on-snow events with flood-generation potential. *Hydrol. Earth Syst. Sci.* **18**, 2695–2709 (2014).
71. Li, D., Lettenmaier, D. P., Margulis, S. A. & Andreadis, K. The role of rain-on-snow in flooding over the conterminous United States. *Water Resour. Res.* **55**, 8492–8513 (2019).
72. Mann, H. Nonparametric tests against trend. *J. Econom. Soc*. **13**, 245–259 (1945).
73. Kendall, M. G. Rank correlation methods, 4th edn (Charles Griffin, London, 1975).
74. Takens, F. Detecting strange attractors in turbulence. In: *Dynamical Systems and Turbulence, Warwick 1980*, Vol. 898 (eds Rand, D. & Young, L. S.) (Springer, Berlin, Heidelberg, 1981).
75. Rasiya Koya, S. Data for 'Northern Pacific Sea-level Pressure Controls Rain-on-Snow in North America'. *Zenodo* https://doi.org/10.5281/zenodo.10956598 (2024).

Acknowledgements

The authors acknowledge the computing resources provided by the Holland Computing Center (HCC) at the University of Nebraska-Lincoln.

Author contributions

S.R.K., K.K.K., and T.R. conceptualized the study. S.R.K. conducted the analysis. S.R.K. and K.K.K. did the data acquisition and preprocessing. S.R.K. prepared the manuscript with inputs from K.K.K., and T.R. T.R. supervised the work.

Competing interests

The authors declare no competing interests.

Additional information

Supplementary information The online version contains supplementary material available at https://doi.org/10.1038/s43247-024-01431-6.

Correspondence and requests for materials should be addressed to Tirthankar Roy.

Peer review information *Communications Earth and Environment* thanks the anonymous reviewers for their contribution to the peer review of this work. Primary Handling Editors: Rahim Barzegar, Joe Aslin and Aliénor Lavergne. A peer review file is available.